Hindawi
Journal of Nanomaterials
Volume 2019, Article ID 6307163, 8 pages
https://doi.org/10.1155/2019/6307163

Research Article

Effects of Single Doping and Composite Doping of Yttrium and Antimony on the Structural, Thermodynamic, Mechanical, and Electronic Properties of Mg_2Si by First Principles

Zhonghao Zhou,[1] **Zhen Zhao**,[2] **and Zhi Li**[3]

[1]*Department of Chemistry, Renmin University of China, Beijing 100872, China*
[2]*School of Chemistry and Life Science, Anshan Normal University, Anshan 114007, China*
[3]*School of Materials and Metallurgy, University of Science and Technology Liaoning, Anshan 114051, China*

Correspondence should be addressed to Zhen Zhao; zhaozhenlunwen@yeah.net

Received 28 May 2018; Accepted 15 October 2018; Published 10 March 2019

Academic Editor: Stefano Bellucci

The structural, stability, thermodynamic, mechanical, and electronic properties of Y and Sb doped into Mg_2Si were studied by first principles. The results show that the stable structures are Mg_7Si_4Y, Mg_8Si_4Sb, Mg_6Si_4YSb, and Mg_7Si_4YSb. Mg_8Si_4Sb has the largest ductility among them. Y doping causes strong orbital hybridization between Mg (2p) and Y (4d), while Sb doping causes strong orbital hybridization between Mg (2p), Si (3p), and Sb (5p). However, the thermal conductivity and hardness of Mg_2Si will be reduced by Y and Sb doping. The conductivity of Mg_8Si_4Sb is the best. The anisotropy of the {100}, {010}, and {001} surfaces will increase once doped with Y or Sb. Mg_8Si_4Sb has the highest degree of anisotropy.

1. Introduction

The 6xxx series aluminum alloy is widely used in automobile manufacturing because of its excellent qualities, such as reduced weight and good corrosion resistance [1, 2]. Mg_2Si is the main strengthening phase [3] of the 6xxx series Al alloy, and it possesses a low density and high melting point and impedes grain boundary sliding [4–9]. However, the application of the 6xxx series Al alloy is limited due to its brittleness. This is due to the Mg_2Si phase which is the preferred phase to form coarse Chinese script or dendritic morphology [10–12]. To improve the mechanical properties of Mg_2Si, many alloying elements (such as Bi, As, and Sn [13–20]) are doped. Recently, Y and Sb doping into the Mg_2Si phase was considered. Zhang and Zhang [21] found that the fine modification effect of Y on the primary Mg_2Si phase is better than that of an equal amount of mixed light rare earth, and it can greatly refine the Mg_2Si grains and improve the tensile strength and elongation. Emamy et al. [22] found that the addition of Y increases both the hardness and ultimate tensile strength values of the Al-15%Mg_2Si cast composite. Jiang et al. [23] systematically investigated the modification of in situ-formed Mg_2Si in Mg–Si alloys with yttrium (Y). Ioannou et al. [24] have prepared Sb-doped Mg_2Si compounds through ball milling and a solid-state reaction. Hu et al. [25] found that Sb doping can change the type of Chinese script of Mg_2Si to a fine polygonal shape and decrease the grain sizes. Tani and Kido [26] studied the formation energy and atomic structure of impurities in Mg_2Sn using first-principles plane-wave total energy calculations. The thermoelectric properties of trace Y-doped Mg_2Si crystals have been obtained by experiments, and the total energies of Mg_7Si_4Y, Mg_8Si_3Y, and Mg_8Si_4Y crystals have also been calculated [27]. What are the differences between the single doping and composite doping of Y and Sb? What are the micromechanisms of Y and Sb doping into Mg_2Si? At present, there is no theoretical research on the brittleness of Mg_2Si by Y and Sb codoping as far as we know.

In this work, the structural, thermodynamic, and mechanical properties of Y and Sb doped into Mg_2Si were studied by first principles. It will provide a theoretical

reference for further research on Mg_2Si and 6xxx series aluminum alloys.

1.1. Computational Models and Methods. Mg_2Si has an anti-fluorite (CaF_2) structure [28] (see Figure 1). The atomic coordinates are as follows: Mg (0.25, 0.25, 0.25) and Si (0, 0, 0).

For Y and Sb single doping, the positions of the Mg (or Si) atoms are replaced by Y or Sb, respectively. Despite that both the atom sizes of Y and Sb are larger than those of Mg and Si atoms, to avoid omitting certain configurations, the interpolation Y or Sb atoms into the interval of Mg and Si was considered (see Figure 2).

For the composite doping of Y and Sb, the Mg and (or) Si atoms are replaced by Y and Sb, respectively. Y or Sb enters into the interstitial space of the Mg_2Si cell, and Sb or Y replaces the Mg and (or) Si atoms (see Figure 3).

The hypothetical structures of Y- and Sb doping or codoping Mg_2Si configurations must be optimized. The calculations were performed using the CASTEP package based on the density functional theory (DFT) [29]. The exchange-correlation energy functional was adopted by Perdew, Burke, and Ernzerhof (PBE) from the generalized gradient approximation (GGA) [30]. The plane-wave cutoff energy was set to 340 eV. The Brillouin zone was sampled using a Monkhorst-Pack k-point mesh as follows: $4\times3\times4$ for (j) Mg_8Si_2YSb, (l) Mg_8Si_3YSb, and (m) Mg_8Si_4YSb and the rest are $4\times4\times4$. To find the lowest energy structures of Y- and Sb-doped Mg_2Si phases, we observe the following convergence thresholds for geometry optimization: total energy convergence tolerance 1.0×10^{-5} eV/atom steps, 0.03 eV/Å for maximum force, 0.05 GPa for maximum stress components, and 1×10^{-3} Å for maximum displacement. After the optimization, the electronic properties are calculated. The density of states (DOS) is computed by means of a scheme developed by Ackland, while the DOS calculation is based on a Mülliken population analysis with the relative contribution of each atom.

2. Results and Discussion

2.1. Structures. The optimized lattice parameters of the pure Mg_2Si phase and Y- and Sb-doped Mg_2Si phases are shown in Table 1. It can be seen that the lattice parameters of Mg_2Si are in agreement with the experimental values [31–33]. Y- and Sb-doped Mg_2Si phases have larger lattice parameters and larger volume than the pure Mg_2Si phase. It is due to the lattice distortion of the Mg_2Si phase by Y and (or) Sb doping which possesses a larger atomic radius.

2.2. Thermodynamic Properties. In order to understand the thermodynamic stability of the doped system, we calculated the formation energy and cohesive energy. The calculated formation energy and cohesive energy of the Mg_2Si phase agree well with the calculated values (−25.92 kJ/mol and −271.15 kJ/mol in [34] and −17.7 kJ/mol and −299.27 kJ/mol in [35]). The process of Y and Sb doping of Mg_2Si is outlined in Table 2.

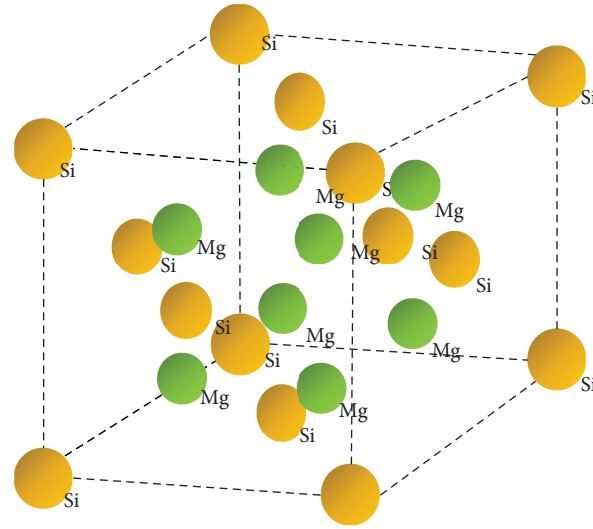

Figure 1: The crystal structure of Mg_2Si.

The corresponding formation energies are shown in Figure 4. It can be seen that the formation energies of (a) Mg_7Si_4Y, (c) Mg_8Si_4Y, (f) Mg_8Si_4Sb, (g) Mg_6Si_4YSb, (i) Mg_7Si_4YSb, (m) Mg_8Si_4YSb, and (n) Mg_7Si_4YSb are negative, indicating that only the structures above are stable. The formation energy is successively (m) < (i) < (n) < (c) < (f) < (g) < (a). It means that (m) Mg_8Si_4YSb is the easiest to form and (a) Mg_7Si_4Y is the most difficult to form. Whether for single doping or composite doping, the formation energies of Y and Sb entered into the interstitial space < the formation energies of Y and Sb replaced the Mg sites < the formation energies of Y and Sb replaced the Si sites (even if it cannot form stable structures). It confirms that Y or Sb is difficult to interpolate into Mg_2Si phases. For the seven stable structures of (a), (c), (f), (g), (i), (m), and (n), the formation energies of composite doping are generally smaller than those of single doping. Only the formation of (g) Mg_6Si_4YSb is greater than those of (c) Mg_8Si_4Y and (f) Mg_8Si_4Sb; this is because Y and Sb in (g) Mg_6Si_4YSb has replaced all the Mg sites to form substitutional solid solutions.

For the stable structures (a), (c), (f), (g), (i), (m), and (n), the calculated cohesive energies are shown in Figure 5. It can be seen that the absolute value of (g) Mg_6Si_4YSb is the largest, indicating that (g) Mg_6Si_4YSb is more stable than the other six structures and (m) Mg_8Si_4YSb has the smallest absolute value and the worst stability. Whether by single doping or composite doping, the structures of Y- or Sb-substituted Mg sites are most stable, while the structures of Y or Sb that entered into the interstitial space are most unstable.

2.3. Mechanical Properties. To satisfy the mechanical stability of the formed structures, the elastic constants of Mg_2Si, (a), (c), (f), (g), (i), (m), and (n) are calculated as shown in Table 3. (a) Mg_7Si_4Y, (c) Mg_8Si_4Y, and (f) Mg_8Si_4Sb are still cubic structures, (g) Mg_6Si_4YSb and (m) Mg_8Si_4YSb are transformed into tetragonal structures, and (i) Mg_7Si_4YSb

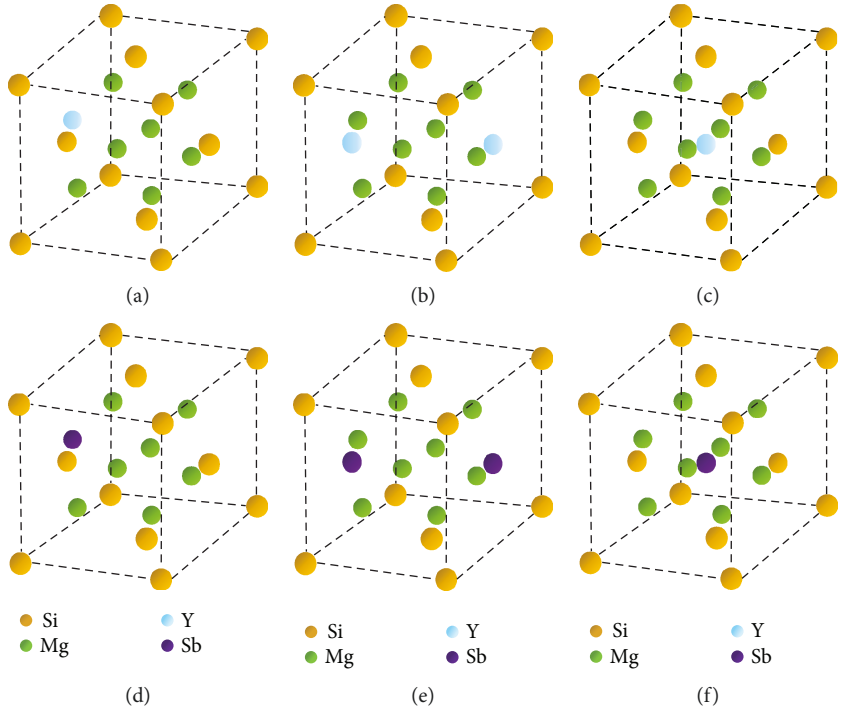

Figure 2: The structures of single doping.

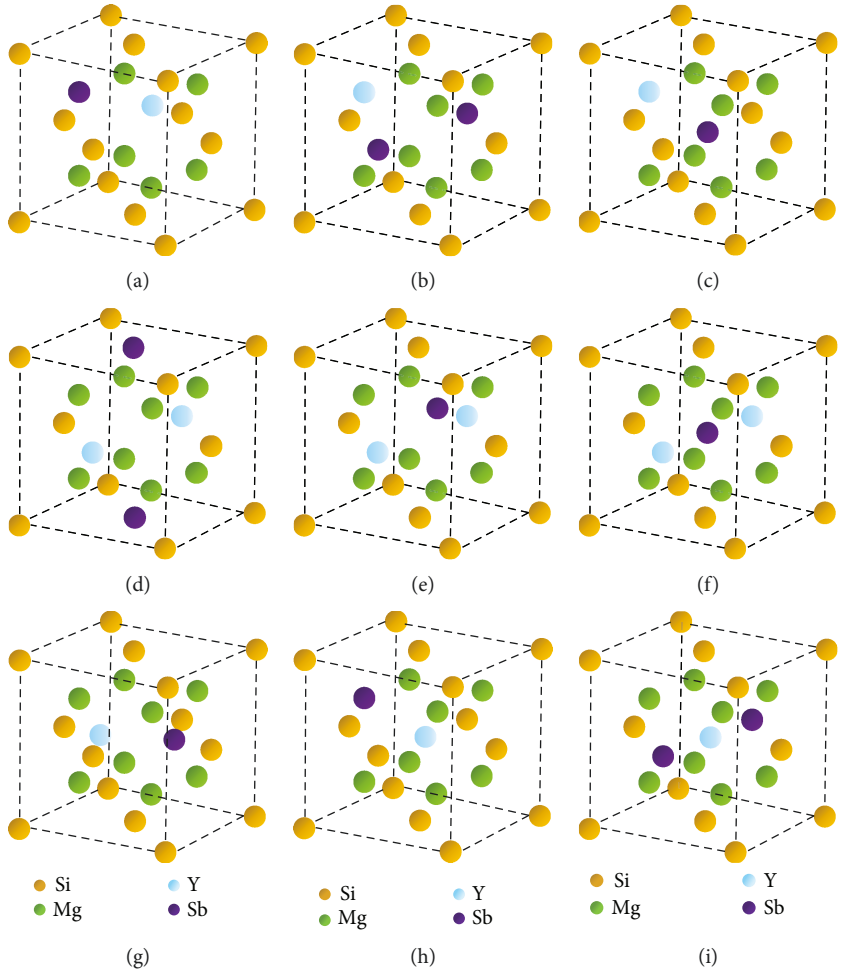

Figure 3: The structures of composite doping.

Table 1: The optimized lattice parameters for Y and (or) Sb doping of Mg_2Si.

Phase	Lattice constants (nm)			Cell volume (nm^3)	Ref.
Mg_8Si_4	$a = 0.633$			$V = 0.254$	
	$a = 0.639$			$V = 0.261$	[31]
	$a = 0.635$			$V = 0.256$	[32]
	$a = 0.634$			$V = 0.255$	[33]
(a) Mg_7Si_4Y	$a = 0.643$			$V = 0.266$	
(b) Mg_8Si_3Y	$a = 0.637$	$b = 0.687$	$c = 0.687$	$V = 0.301$	
(c) Mg_8Si_4Y	$a = 0.653$			$V = 0.278$	
(d) Mg_7Si_4Sb	$a = 0.640$			$V = 0.263$	
(e) Mg_8Si_3Sb	$a = 0.645$	$b = 0.643$	$c = 0.643$	$V = 0.267$	
(f) Mg_8Si_4Sb	$a = 0.656$			$V = 0.282$	
(g) Mg_6Si_4YSb	$a = 0.659$	$b = 0.629$	$c = 0.659$	$V = 0.273$	
(h) Mg_7Si_3YSb	$a = 0.654$	$b = 0.655$	$c = 0.655$	$V = 0.280$	
(i) Mg_7Si_4YSb	$a = 0.662$			$V = 0.290$	
(j) Mg_8Si_2YSb	$a = 0.607$	$b = 0.833$	$c = 0.607$	$V = 0.307$	
(k) Mg_7Si_3YSb	$a = 0.741$	$b = 0.647$	$c = 0.649$	$V = 0.273$	
(l) Mg_8Si_3YSb	$a = 0.615$	$b = 0.820$	$c = 0.604$	$V = 0.304$	
(m) Mg_8Si_4YSb	$a = 0.662$	$b = 0.787$	$c = 0.662$	$V = 0.345$	
(n) Mg_7Si_4YSb	$a = 0.662$			$V = 0.289$	
(o) Mg_8Si_3YSb	$a = 0.643$	$b = 0.690$	$c = 0.661$	$V = 0.293$	

Table 2: The process of Y and Sb doping of Mg_2Si.

Reactants				Products		
Mg_8Si_4	Y		→	(a) Mg_7Si_4Y	Mg	
Mg_8Si_4	Y		→	(b) Mg_8Si_3Y	Si	
Mg_8Si_4	Y		→	(c) Mg_8Si_4Y		
Mg_8Si_4	Sb		→	(d) Mg_7Si_4Sb	Mg	
Mg_8Si_4	Sb		→	(e) Mg_8Si_3Sb	Si	
Mg_8Si_4	Sb		→	(f) Mg_8Si_4Sb		
Mg_8Si_4	Y	Sb	→	(g) Mg_6Si_4YSb	Mg	Mg
Mg_8Si_4	Y	Sb	→	(h) Mg_7Si_3YSb	Mg	Si
Mg_8Si_4	Y	Sb	→	(i) Mg_7Si_4YSb	Mg	
Mg_8Si_4	Y	Sb	→	(j) Mg_8Si_2YSb	Si	Si
Mg_8Si_4	Y	Sb	→	(k) Mg_7Si_3YSb	Mg	Si
Mg_8Si_4	Y	Sb	→	(l) Mg_8Si_3YSb	Si	
Mg_8Si_4	Y	Sb	→	(m) Mg_8Si_4YSb		
Mg_8Si_4	Y	Sb	→	(n) Mg_7Si_4YSb	Mg	
Mg_8Si_4	Y	Sb	→	(o) Mg_8Si_3YSb	Si	

and (n) Mg_7Si_4YSb are transformed into triclinic structures. The mechanical stability of the phases above can be judged by the criterion for cubic, tetragonal, and triclinic systems in References [36] and [37]. Only Mg_2Si, (a) Mg_7Si_4Y, (f) Mg_8Si_4Sb, (g) Mg_6Si_4YSb, and (i) Mg_7Si_4YSb satisfies the criteria of mechanical stability.

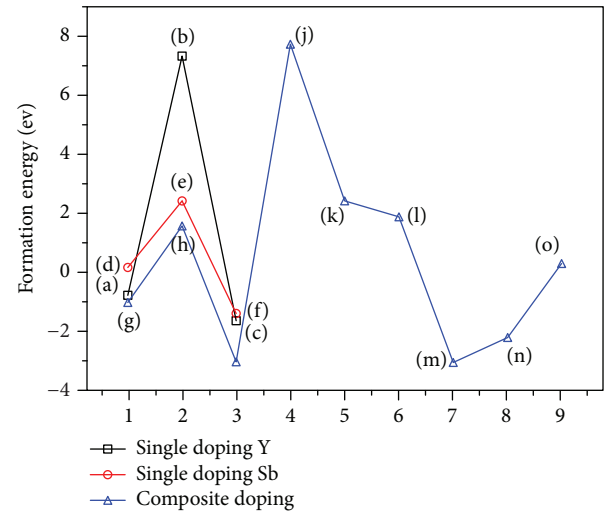

Figure 4: The formation energies of single doping and composite doping.

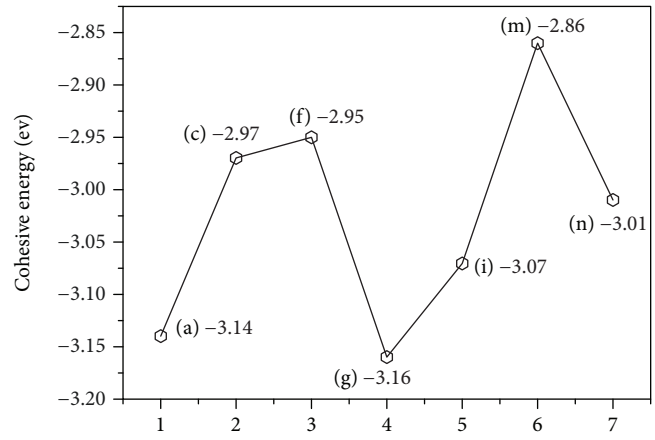

Figure 5: The cohesive energies of single doping and composite doping.

The calculated bulk modulus, shear modulus, and Young's modulus (51.23 GPa, 51.50 GPa, and 115.85 GPa) of Mg_2Si agree well with the calculated results (57.88 GPa, 48.82 GPa, and 114.32 GPa [38]). Young's modulus calculated for Mg_2Si, (a) Mg_7Si_4Y, (f) Mg_8Si_4Sb, (g) Mg_6Si_4YSb, and (i) Mg_7Si_4YSb are shown in Figure 6. No matter with what kind of doping, Young's modulus of pure Mg_2Si will decrease significantly. It means that Mg_2Si has the highest stiffness. In other words, Y and Sb doping will improve the plasticity of Mg_2Si. For single doping, Young's modulus of doped Sb is lesser than that of doped Y. This shows that the plasticity of (f) Mg_8Si_4Sb is better than that of (a) Mg_7Si_4Y, and the stiffness of (a) Mg_7Si_4Y is larger than that of (f) Mg_8Si_4Sb. For composite doping, Young's modulus of (g) Mg_6Si_4YSb is less than Young's modulus of (i) Mg_7Si_4YSb. This shows that the plasticity of (g) Mg_6Si_4YSb is better than that of (i) Mg_7Si_4YSb, and the stiffness of (g) Mg_6Si_4YSb is lesser than that of (i) Mg_7Si_4YSb.

The values of K/G, Poisson's ratio u, A_U, and Debye temperature Θ_D for Mg_2Si, (a) Mg_7Si_4Y, (f) Mg_8Si_4Sb, (g)

Table 3: The elastic constants for Mg_2Si, (a) Mg_7Si_4Y, (c) Mg_8Si_4Y, (f) Mg_8Si_4Sb, (g) Mg_6Si_4YSb, (i) Mg_7Si_4YSb, (m) Mg_8Si_4YSb, and (n) Mg_7Si_4YSb.

Phases	Elastic stiffness constants C_{ij} (GPa)					
Mg_2Si	$C_{11} = 131.31$	$C_{12} = 11.19$	$C_{44} = 46.46$			
(a) Mg_7Si_4Y	$C_{11} = 106.00$	$C_{12} = 25.76$	$C_{44} = 29.00$			
(c) Mg_8Si_4Y	$C_{11} = 22.72$	$C_{12} = 60.54$	$C_{44} = 21.17$			
(f) Mg_8Si_4Sb	$C_{11} = 53.73$	$C_{12} = 40.66$	$C_{44} = 16.16$			
(g) Mg_6Si_4YSb	$C_{11} = 99.10$	$C_{12} = 26.56$	$C_{13} = 28.41$	$C_{33} = 99.21$	$C_{44} = 13.71$	$C_{66} = 13.03$
(i) Mg_7Si_4YSb	$C_{11} = 96.36$	$C_{12} = 23.99$	$C_{13} = 24.26$	$C_{14} = -1.44$	$C_{15} = 2.91$	$C_{16} = -1.61$
	$C_{21} = 23.99$	$C_{22} = 96.44$	$C_{23} = 24.34$	$C_{24} = -1.78$	$C_{25} = 2.58$	$C_{26} = -1.05$
	$C_{31} = 24.26$	$C_{32} = 24.34$	$C_{33} = 96.63$	$C_{34} = -1.17$	$C_{35} = 1.69$	$C_{36} = -1.56$
	$C_{41} = -1.44$	$C_{42} = -1.78$	$C_{43} = -1.17$	$C_{44} = 21.21$	$C_{45} = -0.91$	$C_{46} = 1.69$
	$C_{51} = 2.91$	$C_{52} = 2.58$	$C_{53} = 1.69$	$C_{54} = -0.91$	$C_{55} = 19.72$	$C_{56} = -2.92$
	$C_{61} = -1.61$	$C_{62} = -1.05$	$C_{63} = -1.56$	$C_{64} = 1.69$	$C_{65} = -2.92$	$C_{66} = 20.75$
(m) Mg_8Si_4YSb	$C_{11} = 75.12$	$C_{12} = 20.81$	$C_{13} = 34.21$	$C_{33} = 75.02$	$C_{44} = -11.73$	$C_{66} = -9.39$
(n) Mg_7Si_4YSb	$C_{11} = 52.86$	$C_{12} = 50.91$	$C_{13} = 51.14$	$C_{14} = -8.13$	$C_{15} = -3.89$	$C_{16} = 3.88$
	$C_{21} = 50.91$	$C_{22} = 53.37$	$C_{23} = 52.35$	$C_{24} = 2.55$	$C_{25} = 8.78$	$C_{26} = 1.21$
	$C_{31} = 51.14$	$C_{32} = 52.35$	$C_{33} = 52.71$	$C_{34} = 0.13$	$C_{35} = -0.49$	$C_{36} = -8.16$
	$C_{41} = -8.13$	$C_{42} = 2.55$	$C_{43} = 0.13$	$C_{44} = 21.38$	$C_{45} = -4.73$	$C_{46} = 4.06$
	$C_{51} = -3.89$	$C_{52} = 8.78$	$C_{53} = -0.49$	$C_{54} = -4.73$	$C_{55} = 19.08$	$C_{56} = -3.33$
	$C_{61} = 3.88$	$C_{62} = 1.21$	$C_{63} = -8.16$	$C_{64} = 4.06$	$C_{65} = -3.33$	$C_{66} = 18.76$

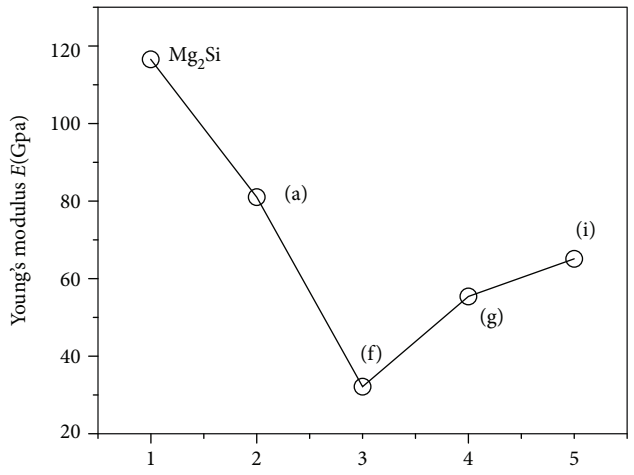

Figure 6: The results of Young's modulus.

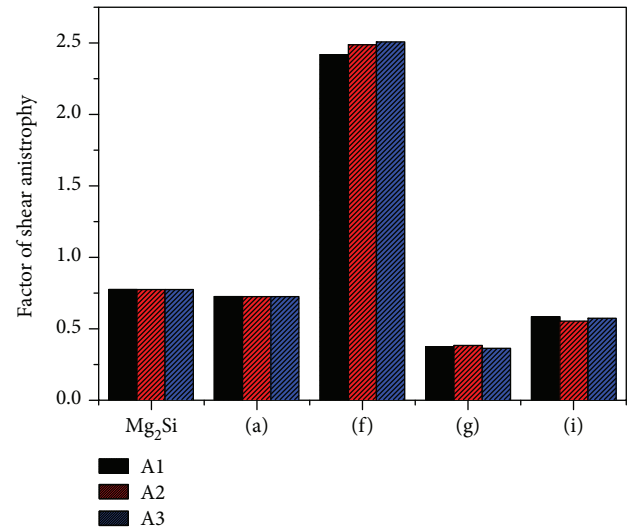

Figure 7: The results of shear anisotropy.

Table 4: The values of the K/G, u, A_U, and Θ_D for Mg_2Si, (a) Mg_7Si_4Y, (f) Mg_8Si_4Sb, (g) Mg_6Si_4YSb, and (i) Mg_7Si_4YSb.

	Mg_2Si	(a) Mg_7Si_4Y	(f) Mg_8Si_4Sb	(g) Mg_6Si_4YSb	(i) Mg_7Si_4YSb
K/G	0.99	1.59	3.99	2.53	1.88
u	0.12	0.24	0.38	0.33	0.27
A_U	7.93	12.85	104.51	138.31	49.18
Θ_D (K)	600.23	445.60	248.77	331.88	346.11

Mg_6Si_4YSb, and (i) Mg_7Si_4YSb are shown in Table 4. Poisson's ratio u (0.12) and Debye temperature Θ_D (600.23 K) calculated for Mg_2Si agree with the results (0.161 and 581.6719 K [38]). From the values of K/G, it can be seen that the values of Mg_2Si and (a) Mg_7Si_4Y are less than the threshold value of 1.75, so Mg_2Si and (a) Mg_7Si_4Y are brittle materials, while (f) Mg_8Si_4Sb, (g) Mg_6Si_4YSb, and (i) Mg_7Si_4YSb are ductile materials. Mg_2Si has minimal K/G and has the worst brittleness, while (f) Mg_8Si_4Sb has maximalK/G and

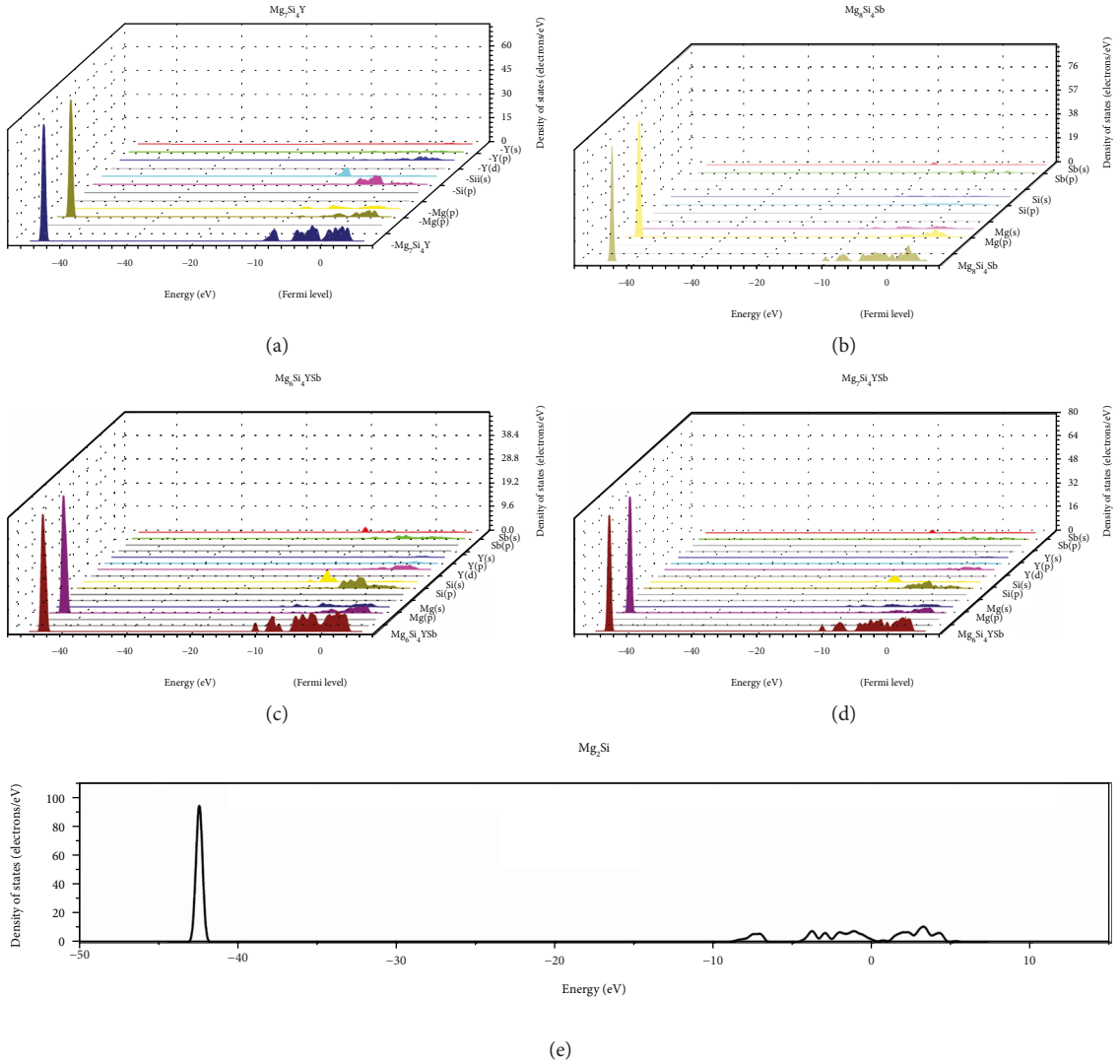

Figure 8: The total density of states (DOS) and the partial density of states (PDOS) for five structures.

has the greatest ductility. From the values of u, it can be seen that (f) Mg_8Si_4Sb has the best plasticity and Mg_2Si has the worst plasticity. The plasticity is successively (f) Mg_8Si_4Sb > (g) Mg_6Si_4YSb > (i) Mg_7Si_4YSb > (a) Mg_7Si_4Y > Mg_2Si. From A_U, it can be seen that the five structures are all anisotropic and Mg_2Si has minimal value, so the degree of anisotropy is minimal. (g) Mg_6Si_4YSb has maximal value, and the degree of anisotropy is the highest. The degree of anisotropy of Mg_2Si will be raised by doped Y and Sb. From the values of Θ_D, it can be seen that the Debye temperature (Θ_D) of Mg_2Si is the highest, which shows that the thermal conductivity of Mg_2Si is the best, the chemical bonds between the cell's atoms are the strongest, and the hardness is the greatest. (f) Mg_8Si_4Sb has the lowest Debye temperature (Θ_D), which shows that the thermal conductivity of (f) Mg_8Si_4Sb is the worst, the chemical bonds between the cell's atoms are the weakest, and the hardness is the least. Furthermore, no matter with what kind of doping, the Debye temperature (Θ_D) of Mg_2Si will be lowered. It is consistent with the calculated results of Debye temperature (Θ_D) [27].

The shear anisotropic factors A_1, A_2, and A_3 are shown in Figure 7. It can be found that the five structures are all anisotropic on the three planes, and the degree of anisotropy on each plane is very similar. (f) Mg_8Si_4Sb has the highest degree of anisotropy, while Mg_2Si has the lowest degree of anisotropy.

2.4. Electronic Properties. To understand the action mechanism, the total density of states (DOS) and the partial density of states (PDOS) should be studied. Figure 8(a) shows the density of states of Mg_7Si_4Y, between −3 eV and the Fermi level, where there exists a very strong orbital hybridization for Mg (2p) and Y (4d) indicating very strong bonding effects. Figure 8(b) shows the density of states of Mg_8Si_4Sb, where there is strong orbital hybridization between the atoms of Mg, Si, and Sb. Figure 8(c) shows the density of states of Mg_6Si_4YSb. The mainly orbital hybridization appears in −6 to 4 eV. The atoms of Mg and Y have strong bonding effects, while the bonding effects of the other atoms are weak. Figure 8(d) shows the

density of states of Mg_7Si_4YSb, where all the four atoms show orbital hybridization. In a word, Y doping causes strong orbital hybridization between Mg (2p) and Y (4d), while Sb doping causes strong orbital hybridization between Mg (2p), Si (3p), and Sb (5p). The Fermi surface shifts towards the high-energy region after Y and Sb doping, resulting in an increase in the density of the electron energy states corresponding to the Fermi level. The values are 2 eV (Mg_2Si), 3.05 eV (Mg_7Si_4Y), 5.4 eV (Mg_8Si_4Sb), 3.7 eV (Mg_6Si_4YSb), and 2.9 eV (Mg_7Si_4YSb) in turn, indicating that doping can improve the electrical conductivity of Mg_2Si. This is also consistent with the results which were obtained in Reference [27]. The electrical conductivity of Mg_8Si_4Sb is the best.

3. Conclusions

The structural, stability, thermodynamic, and mechanical properties of Y and Sb doped into Mg_2Si are calculated by the GGA-PBE method. The results revealed that the stable structures that can be formed are (a) Mg_7Si_4Y, (f) Mg_8Si_4Sb, (g) Mg_6Si_4YSb, and (i) Mg_7Si_4YSb. (g) Mg_6Si_4YSb is the most stable, while (f) Mg_8Si_4Sb is the least stable. Young's modulus of Mg_2Si will be reduced by Y and Sb doping, the ductility of Mg_2Si will be improved, and the brittleness of Mg_2Si will be well solved. Among them, the effect of single-doped Sb is better. The Debye temperature (Θ_D) of Mg_2Si will be lowered, and then the thermal conductivity and hardness of Mg_2Si will be reduced by Y and Sb doping. The Debye temperature (Θ_D) of (f) Mg_8Si_4Sb in the five structures is the lowest. Doping with Y and Sb can improve the conductivity of Mg_2Si, and Mg_8Si_4Sb has the best conductivity.

Data Availability

The computational data used to support the findings of this study are included within the article.

Conflicts of Interest

The authors declare that there is no conflict of interest regarding the publication of this paper.

Acknowledgments

The authors would like to acknowledge the National Natural Science Foundation of China. This work was also supported by the Key Fund Project (Grant No. 51634004), the Doctoral Scientific Research Foundation of Liaoning Province (Grant No. 20180551213), the Key Laboratory of Chemical Metallurgy Engineering of Liaoning Province, University of Science and Technology Liaoning (Grant No. USTLKFSY201711), and the Fund Project of University of Science and Technology Liaoning (Grant No. 2017YY02).

References

[1] M. Hosseinifar and D. V. Malakhov, "Effect of Ce and La on microstructure and properties of a 6xxx series type aluminum alloy," *Journal of Materials Science*, vol. 43, no. 22, pp. 7157–7164, 2008.

[2] O. Engler, C. Schäfer, and H. J. Brinkman, "Crystal-plasticity simulation of the correlation of microtexture and roping in AA 6xxx Al–Mg–Si sheet alloys for automotive applications," *Acta Materialia*, vol. 60, no. 13-14, pp. 5217–5232, 2012.

[3] A. Jahangiri, M. H. Idris, and S. Farahany, "Investigation on tungsten inert gas welding of in situ Al-15 and 20 Mg_2Si composites with an Al-Si filler," *Journal of Composite Materials*, vol. 47, no. 10, pp. 1283–1291, 2013.

[4] B. Yu, D. Chen, Q. Tang, C. Wang, and D. Shi, "Structural, electronic, elastic and thermal properties of Mg_2Si," *Journal of Physics and Chemistry of Solids*, vol. 71, no. 5, pp. 758–763, 2010.

[5] H. Y. Wang, Q. C. Jiang, B. X. Ma, Y. Wang, J. G. Wang, and J. B. Li, "Modification of Mg_2Si in Mg–Si alloys with K_2TiF_6, KBF_4 and $KBF_4 + K_2TiF_6$," *Journal of Alloys and Compounds*, vol. 387, no. 1-2, pp. 105–108, 2005.

[6] L. Wang and X. Y. Qin, "The effect of mechanical milling on the formation of nanocrystalline Mg_2Si through solid-state reaction," *Scripta Materialia*, vol. 49, no. 3, pp. 243–248, 2003.

[7] J. Zhang, Z. Fan, Y. Q. Wang, and B. L. Zhou, "Microstructural development of Al–15wt.%Mg_2Si in situ composite with mischmetal addition," *Materials Science and Engineering: A*, vol. 281, no. 1-2, pp. 104–112, 2000.

[8] M. Emamy, H. R. Jafari Nodooshan, and A. Malekan, "The microstructure, hardness and tensile properties of Al–15%Mg_2Si in situ composite with yttrium addition," *Materials & Design*, vol. 32, no. 8-9, pp. 4559–4566, 2011.

[9] Y.-Z. Lü, Q.-D. Wang, X.-Q. Zeng, W.-J. Ding, and Y.-P. Zhu, "Effects of silicon on microstructure, fluidity, mechanical properties, and fracture behaviour of Mg–6Al alloy," *Materials Science and Technology*, vol. 17, no. 2, pp. 207–214, 2001.

[10] A. Bahrami, A. Razaghian, M. Emamy, and R. Khorshidi, "The effect of Zr on the microstructure and tensile properties of hot-extruded Al–Mg_2Si composite," *Materials & Design*, vol. 36, pp. 323–330, 2012.

[11] N. Soltani, A. Bahrami, and M. I. Pech-Canul, "The effect of Ti on mechanical properties of extruded in-situ Al-15 pct Mg_2Si composite," *Metallurgical and Materials Transactions A*, vol. 44, no. 9, pp. 4366–4373, 2013.

[12] H. Z. Ye and X. Y. Liu, "Review of recent studies in magnesium matrix composites," *Journal of Materials Science*, vol. 39, no. 20, pp. 6153–6171, 2004.

[13] V. K. Zaitsev, M. I. Fedorov, E. A. Gurieva et al., "Highly effective Mg_2Si_{1-x} Sn_x thermoelectrics," *Physical Review B*, vol. 74, no. 4, article 045207, 2006.

[14] W. Liu, Q. Zhang, X. Tang, H. Li, and J. Sharp, "Thermoelectric properties of Sb-doped $Mg_2Si_{0.3}Sn_{0.7}$," *Journal of Electronic Materials*, vol. 40, no. 5, pp. 1062–1066, 2011.

[15] J. Tani and H. Kido, "First-principles and experimental studies of impurity doping into Mg_2Si," *Intermetallics*, vol. 16, no. 3, pp. 418–423, 2008.

[16] T. Sakamoto, T. Iida, S. Kurosaki et al., "Thermoelectric behavior of Sb- and Al-doped n-type Mg_2Si device under large temperature differences," *Journal of Electronic Materials*, vol. 40, no. 5, pp. 629–634, 2011.

[17] T. Sakamoto, T. Iida, A. Matsumoto et al., "Thermoelectric characteristics of a commercialized Mg_2Si source doped with Al, Bi, Ag, and Cu," *Journal of Electronic Materials*, vol. 39, no. 9, pp. 1708–1713, 2010.

[18] M. I. Fedorov, V. K. Zaitsev, I. S. Eremin et al., "Kinetic properties of p-type $Mg_2Ge_{0.4}Sn_{0.6}$ solid solutions," in *Proceedings of the 2nd European Conference on Thermoelectrics*, Krakow, Poland, 2004.

[19] M. C. Nicolaou, "Preparation, doping, physical properties and applications of the semiconductor solid solutions $Mg_2Si_xGe_ySn_{1-x-y}$," in *Proceedings of 5th International Conference on Thermoelectric Energy Conversion*, Arlington, TX, USA, 2005.

[20] J. J. Pulikkotil, H. N. Alshareef, and U. Schwingenschlogl, "Fast track communication: variation of equation of state parameters in the $Mg_2(Si_{1-x}Sn_x)$ alloys," *Journal of Physics: Condensed Matter*, vol. 22, no. 35, article 352204, 2010.

[21] A. S. Zhang and Y. Zhang, "Effect of RE, yttrium on morphology of primary Mg_2Si phases in Mg_2Si/AZ91D composites," *Special Casting & Nonferrous Alloys*, vol. 32, no. 8, pp. 690–693, 2012.

[22] M. C. Nicolaou, "Preparation, doping, physical properties and applications of the semiconductor solid solutions Mg2Six-GeySn1-x-y," in *Proceedings of 5th International Conference on Thermoelectric Energy Conversion*, Arlington, TX, USA, 2005.

[23] Q. C. Jiang, H. Y. Wang, Y. Wang, B. X. Ma, and J. G. Wang, "Modification of Mg_2Si in Mg–Si alloys with yttrium," *Materials Science & Engineering A*, vol. 392, no. 1-2, pp. 130–135, 2005.

[24] M. Ioannou, G. Polymeris, E. Hatzikraniotis, A. U. Khan, K. M. Paraskevopoulos, and T. Kyratsi, "Solid-state synthesis and thermoelectric properties of Sb-doped Mg_2Si materials," *Journal of Electronic Materials*, vol. 42, no. 7, pp. 1827–1834, 2013.

[25] Y. Hu, L. Rao, and H. Yan, "Microstructures and mechanical properties of Si and Sb added Mg alloy," *Applied Mechanics and Materials*, vol. 44-47, pp. 2809–2813, 2011.

[26] J. Tani and H. Kido, "Impurity doping into Mg_2Sn: a first-principles study," *Physica B: Condensed Matter*, vol. 407, no. 17, pp. 3493–3498, 2012.

[27] W. Fan, R. Chen, L. Wang, P. Han, and Q. Meng, "First-principles and experimental studies of Y-doped Mg_2Si prepared using field-activated pressure-assisted synthesis," *Journal of Electronic Materials*, vol. 40, no. 5, pp. 1209–1214, 2011.

[28] P. Villars and L. D. Calvert, *Handbook of Crystallographic Data for Intermetallic Phases*, ASM International, Metals Park, OH, USA, 2nd edition, 1991.

[29] Z. W. Huang, Y. H. Zhao, H. Hou et al., "Point defects structure and alloying effects of V atoms into Ni_3Al alloy: a first-principles study," *Rare Metal Materials and Engineering*, vol. 40, no. 12, pp. 2136–2141, 2011.

[30] J. P. Perdew, K. Burke, and M. Ernzerhof, "Generalized gradient approximation made simple," *Physical Review Letters*, vol. 77, no. 18, pp. 3865–3868, 1996.

[31] E. A. Owen and G. D. Preston, "The atomic structure of two intermetallic compounds," *Proceedings of the Physical Society of London*, vol. 36, no. 1, pp. 341–348, 1924.

[32] J. G. Barlock and L. F. Mondolfo, "Structure of some aluminium-iron-magnesium-manganese-silicon alloys," *Zeitschrift für Metallkunde*, vol. 66, p. 605, 1975.

[33] V. M. Glazov and N. N. Glagoleva, "Change in the nature of the chemical bond in compounds of magnesium with Si, Ge, Sn, and Pb upon melting," *Inorganic Materials*, vol. 1, p. 989, 1965.

[34] L. Zhang, H. Hou, Z. Wen, and Y. Guo, "Electronic structural, elastic properties of $MgCu_2$ and Mg_2Si phases based on first-principles calculation," *Journal of Measurement Science and Instrumentation*, vol. 8, no. 3, pp. 289–294, 2017.

[35] H. Zhang, S. Shang, J. E. Saal et al., "Enthalpies of formation of magnesium compounds from first-principles calculations," *Intermetallics*, vol. 17, no. 11, pp. 878–885, 2009.

[36] Z. J. Wu, E. J. Zhao, H. P. Xiang, X. F. Hao, X. J. Liu, and J. Meng, "Crystal structures and elastic properties of superhard Ir N_2 and Ir N_3 from first principles," *Physical Review B*, vol. 76, no. 5, article 054115, 2007.

[37] F. Mouhat and F. X. Coudert, "Necessary and sufficient elastic stability conditions in various crystal systems," *Physical Review B*, vol. 90, no. 22, article 224104, 2014.

[38] Z. W. Huang, Y. H. Zhao, H. Hou, and P. D. Han, "Electronic structural, elastic properties and thermodynamics of $Mg_{17}Al_{12}$, Mg_2Si and Al_2Y phases from first-principles calculations," *Physica B: Condensed Matter*, vol. 407, no. 7, pp. 1075–1081, 2012.